Quantifying resonance behavior in the fusion of ¹⁷O with ¹²C at above-barrier energies

S. Hudan, J. E. Johnstone, Rohit Kumar, and R. T. deSouza

Department of Chemistry and Center for Exploration of Energy and Matter, Indiana University 2401 Milo B. Sampson Lane, Bloomington, Indiana 47408, USA

J. Allen, D. W. Bardayan, D. Blankstein, C. Boomershine, S. Carmichael, A. Clark, S. Coil, S. L. Henderson, P. D. O'Malley, and W. W. von Seeger

Department of Physics, University of Notre Dame, Notre Dame, Indiana 46556, USA

(Received 17 April 2023; accepted 7 June 2023; published 26 June 2023)

Recent measurement of the fusion excitation function for $^{17}\mathrm{O} + ^{12}\mathrm{C}$ reported the significant suppression of the fusion cross section at $E_{\mathrm{c.m.}} \approx 14$ MeV. This suppression was hypothesized to signal the existence of a $^{16}\mathrm{O} + n + ^{12}\mathrm{C}$ molecular configuration. Using the active-target detector MuSIC@Indiana provided an effective means of reexamining the fusion excitation function for $^{17}\mathrm{O} + ^{12}\mathrm{C}$. The accuracy of this thick-target measurement is strengthened through comparison with the thin-target measurement of the excitation function for $^{17}\mathrm{F} + ^{12}\mathrm{C}$. The result provides important information about the dependence of the average fusion cross section for the oxygen isotopic chain on neutron excess.

DOI: 10.1103/PhysRevC.107.064612

I. INTRODUCTION

Fusion is an interesting process in which two nuclei, small quantal systems, merge to form a larger nucleus. The process is governed by an interaction barrier resulting from the delicate balance of repulsive Coulomb and attractive nuclear forces between the two nuclei. As the two nuclei approach and merge, mutual excitation of the two nuclei occurs. These intrinsic excitations are accompanied by changes in the shape of the two nuclei, i.e., collective modes. This coupling between intrinsic and collective modes can play an important role in the fusion process, where coherent couplings between the colliding nuclei can be magnified [1]. Consequently, lowenergy fusion is sensitive to the structure of the reacting nuclei [2]. At low energies an indirect window into fusion is provided by examination of elastic scattering. Measurement of the elastic scattering cross section in ${}^{12}C + {}^{12}C$ revealed significant resonant behavior. These resonances were attributed to the formation of "molecular complexes" between the two nuclei [3]. As fusion is the dominant reaction channel at the incident energies measured, one might expect that the resonant behavior in the elastic channel should be correlated with changes in the fusion excitation function. Resonant behavior was clearly observed in the fusion excitation function of ${}^{16}O + {}^{12}C$ [4–6]. Recently, a large decrease of ≈200 mb in the fusion cross section of $^{17}\text{O} + ^{12}\text{C}$ at $E_{\text{c.m.}} \approx 14$ MeV was reported [7]. The authors linked this suppression to the well known oscillatory structures in $^{16}\text{O} + ^{12}\text{C}$. They hypothesized that the occurrence of constructive and destructive interference resulted from formation of a ${}^{16}\text{O} + n + {}^{12}\text{C}$ type configuration [7]. This conclusion is highly interesting, justifying the remeasurement of this reaction.

A particular challenge in measuring $^{17}\mathrm{O} + ^{12}\mathrm{C}$ is the low natural abundance of $^{17}\mathrm{O}$ (0.038%) motivating use of a thick-target technique. Recent development of active thick-target approaches facilitate the measurement of low-energy fusion excitation functions with low-intensity beams of either radioactive or stable species. Specifically, by employing a multisampling ionization chamber (MuSIC), direct detection of the heavily-ionizing reaction products can be achieved [8–10]. Validating the accuracy of the thick-target fusion excitation function is essential and requires suitable comparison with conventional thin-target measurements.

II. MuSIC@Indiana

A MuSIC detector is a simple, active thick-target detector. It consists of a transverse-field, Frisch-gridded ionization chamber with the anode subdivided into strips transverse to the beam direction. The signal from each anode segment is independently read out, allowing the energy deposit of an ionizing particle to be sampled along the beam direction. As it traverses the detector, the incident beam loses energy in the gas at a rate characterized by its specific ionization. If a fusion event occurs, amalgamation of the projectile and target nuclei results in a compound nucleus (CN) with larger atomic and mass number than the incident beam. At modest excitation the CN deexcites to form an evaporation residue (ER) which still manifests an increased atomic and mass number as compared to the beam. Due principally to its greater atomic number, the specific ionization of the ER is larger than that of the beam. This increase provides the ability to distinguish the presence of an ER, which signals the occurrence of a fusion event. By determining the position at which fusion occurs within the active volume, multiple energies on the fusion excitation are simultaneously measured for a single incident energy. This

^{*}desouza@indiana.edu

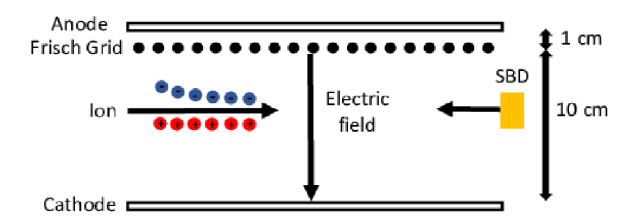


FIG. 1. Schematic side view of MuSIC@Indiana. Insertion of the surface barrier silicon detector (SBD) from downstream into the active volume is also indicated. Taken from [9].

approach thus provides a highly efficient means of measuring the total fusion cross section. As the same detector is used to count both beam and evaporation residues, the method is also self-normalizing.

The overall design of MuSIC@Indiana is similar to other MuSIC detectors presently in use [8,10,11] with some key differences. The active volume of MuSIC@Indiana is formed by six printed circuit boards (PCBs) which together constitute a rectangular box. The top and bottom of the box, with an active area of 25.97 cm × 23.00 cm, serve as the anode and cathode respectively [9]. Between the anode and cathode is a wire plane (50 µm diameter Au-W wires on a 1 mm pitch) that acts as a Frisch grid. A side view of MuSIC@Indiana indicating the anode-to-Frisch grid and Frisch grid-to-cathode spacings is presented in Fig. 1. To provide a short collection time of the primary ionization produced by an incident ion, the detector is operated at a reduced electric field of $\approx 0.7 \text{ kV/(cm atm)}$ between the cathode and the Frisch grid. This field yields an electron drift velocity of ≈ 10 cm/ μ s in CH₄ [12]. A significantly higher reduced electric field between the Frisch grid and the anode [\approx 1.4 kV/(cm atm)] minimizes termination of electrons on the Frisch grid. Field shaping at the edges of the detector is accomplished by enclosing the active volume with four PCBs each having 1.613 mm strips with a center-to-center pitch of 3.226 mm. A 30 mm diameter hole in the upstream and downstream PCBs allows the beam to enter and exit the active volume of the detector. The hole in the downstream PCB also enables the precise insertion of a small silicon surface barrier detector (SBD) using a linear-translation system. This ability to insert a SBD precisely into the active volume is critical in the calibration and operation of MuSIC@Indiana as it allows direct measurement of beam energy at a given location [9].

The anode plane of MuSIC@Indiana consists of twenty anodes. Each anode segment is 1.219 cm wide with a 0.031 cm interstrip separation between anodes. This width for an anode segment along the beam direction was chosen to provide a sufficiently large ΔE signal to yield a good signal-to-noise ratio. When the detector is operated at P=150 torr of CH₄ gas, an incident ¹⁷O ion with $E_{\text{lab}}=50$ MeV deposits a ΔE of ≈ 1.5 MeV for an anode.

III. EXPERIMENTAL DATA

Commissioning experiments with MuSIC@Indiana involved measurement of the fusion excitation function of ¹⁸O + ¹²C [9,13]. The ¹⁸O beam was produced from enriched

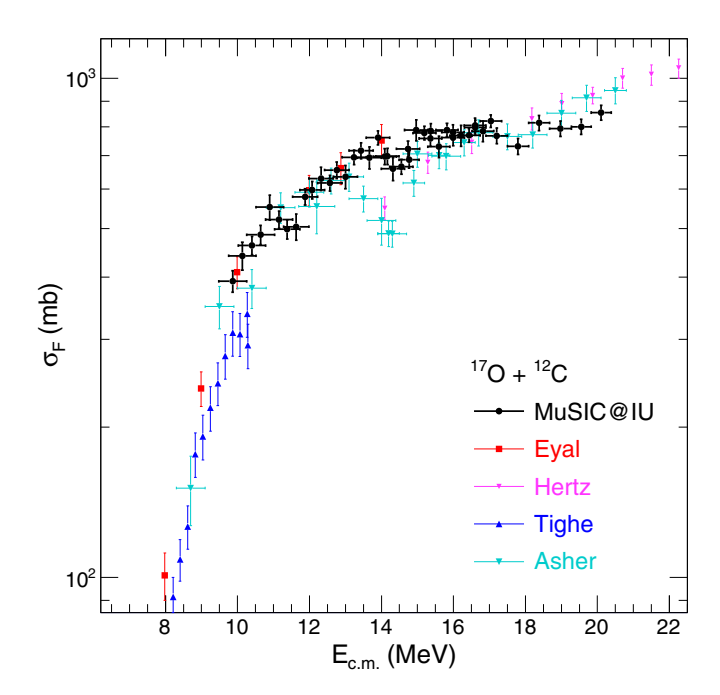


FIG. 2. Excitation function for ${}^{17}O + {}^{12}C$.

source material and the beam intensity was reduced using a sieve to a rate of 10^4 – 10^5 ions/s compatible with MuSIC@Indiana. Comparison of the results of these measurements demonstrated that the thick-target technique was in good agreement with prior thin-target measurements [9,13]. Having established the robustness of the approach, we focused on measurement of the fusion excitation function for $^{17}O + ^{12}C$, where a large decrease in the fusion excitation function at $E_{\rm c.m.} \approx 14$ MeV had been reported by Asher *et al.* [7]. This measurement purported to have resolved a discrepancy in cross section of approximately 200 mb that had existed in the literature for prior thin-target measurements by Eyal et al. [14] and Hertz et al. [15]. In this work we reexamine the large suppression at $E_{\rm c.m.} \approx 14~{\rm MeV}$ as such an interference could be quite interesting as such oscillations can point to specific channel couplings.

The experiment was performed at the University of Notre Dame Nuclear Science Laboratory where a ¹⁷O beam with an intensity of 10⁴ ions/s was produced from natural abundance of oxygen (0.038% ¹⁷O). The beam, accelerated to energies of $E_{lab} = 55$, 48, 47.5, and 47 MeV, impinged on MuSIC@Indiana. The CH₄ gas in MuSIC@Indiana, at a pressure of 150 torr (99.999% purity), served as both target and detection medium. At the incident energies measured, fusion of the incident beam with ¹²C nuclei produces ²⁹Si with an excitation energy $E^* = 40$ –44 MeV. This compound nucleus deexcites by emission of neutrons, protons, and α particles to produce an evaporation residue. Direct measurement of the energy loss for calibration beams of ^{17,18}O, ¹⁹F, ²³Na, ^{24,26}Mg, ²⁷Al, and ²⁸Si meant that the identification of residues did not primarily rely on energy loss calculations, which typically have uncertainties of 10–15% [9,16].

Presented in Fig. 2 is data for fusion of $^{17}\text{O} + ^{12}\text{C}$. The present measurement spans $9.9 \leqslant E_{\text{c.m.}} \leqslant 20.1$ MeV. The

emphasis in the present work of performing a high-quality measurement in the resonance regime is evident. The horizontal error bars of 300 keV correspond to the spatial localization of the fusion event on a single anode. By utilizing small changes in the incident energy a fine mapping of the resonance regime is achieved. Vertical error bars are dominated by the statistical uncertainties. The quality of the statistics in the present measurement precluded utilizing subanode spatial localization [13] which would increase the cross-section uncertainty but would yield a larger number of points. Overall the present data are in good agreement with previously published data. Below $E_{c.m.} = 13$ MeV, the cross sections in this work largely agree, within the reported uncertainties, with those reported by Asher et al. and Eyal et al. For $E_{\rm c.m.} > 18$ MeV the present cross sections lie slightly below those measured by Hertz [15] and Asher [7]. A significant difference is observed at $E_{\rm c.m.} \approx 14$ MeV between the present data and the cross sections recently reported by Asher et al. Compared to Asher *et al.* the dip in the cross section in the present work is considerably smaller in magnitude, approximately 50 mb, and occurs at a slightly higher energy. The present results are consistent with the cross sections previously reported by Eyal et al. while the Asher et al. cross section in the resonance region is consistent with the lowest energy measurement of Hertz et al. [15]. The dips in cross section at $E_{\rm c.m.} \approx 14$ MeV as well as the one at $E_{\rm c.m.} \approx 11$ MeV may have a common origin. Successive l waves result in an increased repulsive potential which produces slightly different barriers and consequently changes in the fusion cross section [17,18]. The present data are of sufficiently high quality to observe these differences.

In order to ascertain the accuracy of the measured cross sections in the resonance region we compared the measured fusion excitation function with that of ${}^{17}F + {}^{12}C$ [19]. Since ¹⁷F and ¹⁷O are mirror nuclei one expects a similar behavior for the fusion excitation function when the difference in Coulomb is accounted for. While at some level the excitation functions with the two mirror nuclei must be different as mirror levels in the two nuclei are slightly different and coupling to the fusion channel will change, nonetheless this is a valuable comparison. Shown in Fig. 3 are the fusion excitation functions for both ¹⁷F and ¹⁷O induced reactions. To compare the two excitation functions appropriately the cross sections are presented relative to the Bass fusion barrier (V_B) [20]. For the ¹⁷O reaction the measured cross sections of the present work together with that of Tighe et al. [21] and Eyal et al. are depicted as the solid gold band. Indicated by the closed (red) symbols is the fusion excitation function [Indiana University (IU)] for ${}^{17}F + {}^{12}C$ [19]. This measurement was a thin-target experiment which utilized an energy/time-offlight approach to identify the ERs. With the exception of the point at $E_{\rm c.m.} - V_B \approx 5$ MeV all of the $^{17}{\rm F}$ (IU) data lie within the gold band. In particular the resonance dips at $E_{\rm c.m.} - V_B \approx 7$ MeV and ≈ 3.5 MeV, corresponding to the dips in the cross section at $E_{\rm c.m.} \approx 14$ MeV and 11 MeV respectively shown in Fig. 2, are well reproduced by the ¹⁷F (IU) data. It is important to note that the large dip in cross section observed by Asher et al. for 17O is not manifested in either ¹⁷F dataset. The measurement

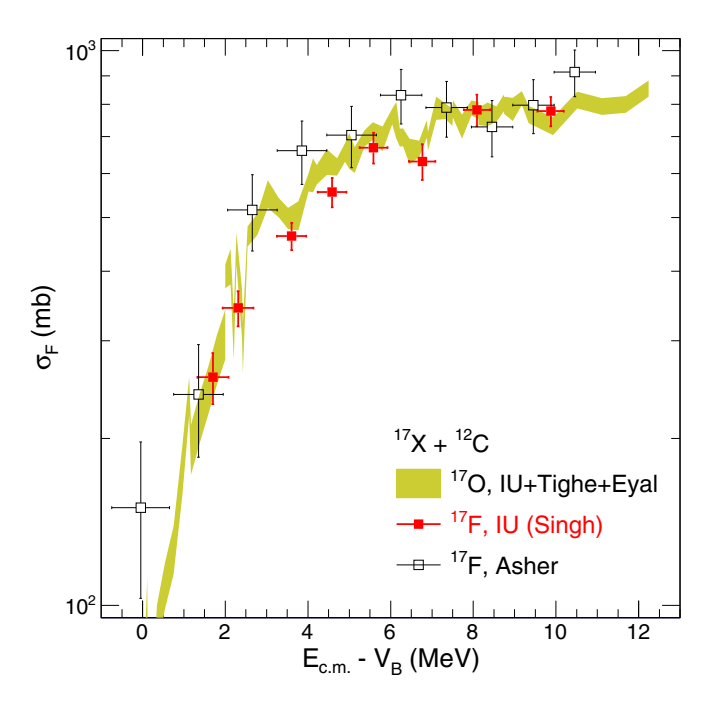


FIG. 3. Comparison of the excitation functions for $^{17}O + ^{12}C$ with the excitation function for $^{17}F + ^{12}C$ measured by IU [19] (closed, red symbols) and Asher *et al.* [10] (open, black symbols).

of $^{17}\text{F} + ^{12}\text{C}$ by Asher *et al.* [10] with a MuSIC detector indicated by the open (black) symbols, though systematically higher is still in reasonable agreement with the measured ^{17}O excitation function. It should be noted that the uncertainties of the Asher *et al.* measurement in both cross section and energy are significantly larger than those of the IU ^{17}F data. This good agreement of the present ^{17}O data with our prior ^{17}F measurement provides confidence in the accuracy of the present measurement of the $^{17}\text{O} + ^{12}\text{C}$ excitation function.

Having extracted an accurate excitation function for $^{17}\mathrm{O} + ^{12}\mathrm{C}$, we calculated the average fusion cross section for the interval $12 \leqslant E_{\mathrm{c.m.}} \leqslant 18$ MeV. The result is compared with the average cross section for $^{16,18,19}\mathrm{O} + ^{12}\mathrm{C}$ as a function of neutron excess, N-Z, in Fig. 4 [22]. The average fusion cross section for $^{17}\mathrm{O}$ is 727 ± 54 mb, lower than that of both adjacent isotopes with paired neutrons. This reduction in average cross section is in marked contrast to the large enhancement observed for $^{19}\mathrm{O}$. All of the valence neutrons for N-Z>0 originate in the sd shell. This suppression of the average fusion cross section for $^{17}\mathrm{O}$ makes the enhancement observed for $^{19}\mathrm{O}$ even more interesting as it suggests that the enhancement for $^{19}\mathrm{O}$ is not solely due to a simple understanding of pairing.

IV. CONCLUSIONS

The fusion excitation function for $^{17}\mathrm{O} + ^{12}\mathrm{C}$ was successfully measured with MuSIC@Indiana using a beam from unenriched material (0.038% natural abundance). The resulting excitation function is in good agreement with multiple datasets in the near-barrier regime. Importantly, however, it did not manifest the large suppression of the fusion cross section at $E_{\mathrm{c.m.}} \approx 14$ MeV reported by Asher *et al.* The

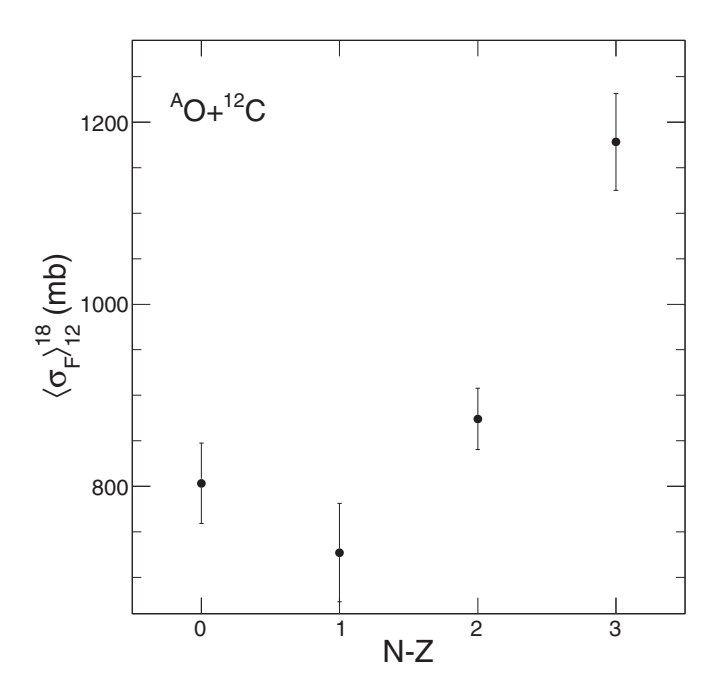


FIG. 4. Dependence of the average fusion cross section for $^{A}O + ^{12}C$ in the energy interval $12 \leqslant E_{\text{c.m.}} \leqslant 18$ MeV as a function of neutron excess, N-Z.

present measurement is therefore inconsistent with the significant suppression at $E_{\text{c.m.}} \approx 14$ MeV, interpreted by Asher *et al.* as evidence for the existence of a $^{16}\text{O} + n + ^{12}\text{C}$

molecular configuration. The present measurement does observe a decrease in the cross section that is considerably smaller in magnitude, \approx 50 mb at $E_{\rm c.m.} \approx 14.5$ MeV. A similar decrease is also observed at $E_{\rm c.m.} \approx 11$ MeV. These dips in the cross section are consistent in magnitude with changes due to the increasing barrier associated with successive l waves. The present ¹⁷O fusion excitation function is also in good agreement with thin-target measurements of the mirror nucleus ¹⁷F when corrected for the difference in Coulomb interaction between the two systems. This agreement of the mirror nuclei further supports the accuracy of the present measurement. The extraction of the average fusion cross section for ¹⁷O provides valuable insight into the trend of the average fusion cross section for the oxygen isotope chain. The reduction of the average fusion cross section for ¹⁷O as compared to ¹⁶O and ¹⁸O underscores that the increase in cross section for $^{19}O + ^{12}C$ is surprising. This indicates that the increase for ¹⁹O cannot be simply understood as a simple pairing effect. Investigation of even more neutron-rich members of the isotopic chain in the near future is anticipated.

ACKNOWLEDGMENTS

We acknowledge the high quality beam provided by the students and staff at the University of Notre Dame that made this experiment possible. This work was supported by the U.S. Department of Energy Office of Science under Grant No. DE-FG02-88ER-40404 (Indiana University) and by the National Science Foundation under Grant No. PHY-2011890 (University of Notre Dame).

^[1] B. B. Back, H. Esbensen, C. L. Jiang, and K. E. Rehm, Rev. Mod. Phys. 86, 317 (2014).

^[2] K. Godbey, A. S. Umar, and C. Simenel, Phys. Rev. C 106, L051602 (2022).

^[3] D. Bromley, J. Kuehner, and E. Almquist, Phys. Rev. Lett. 4, 365 (1960).

^[4] P. Sperr, T. H. Braid, Y. Y. Eisen, D. G. Kovar, F. W. Prosser, J. P. Schiffer, S. L. Tabor, and S. Vigdor, Phys. Rev. Lett. 37, 321 (1976).

^[5] D. G. Kovar et al., Phys. Rev. C 20, 1305 (1979).

^[6] A. D. Frawley, N. R. Fletcher, and L. C. Dennis, Phys. Rev. C 25, 860 (1982).

^[7] B. Asher, S. Almaraz-Calderon, K. Kemper, L. Baby, E. Lopez-Saavedra, A. Morelock, J. Perello, V. Tripathi, and N. Keeley, Eur. Phys. J. A 57, 272 (2021).

^[8] P. F. F. Carnelli *et al.*, Phys. Rev. Lett. **112**, 192701 (2014).

^[9] J. Johnstone *et al.*, Nucl. Instrum. Methods Phys. Res. Sect. A 1014, 165697 (2021).

^[10] B. W. Asher, S. Almaraz-Calderon, V. Tripathi, K. W. Kemper, L. T. Baby, N. Gerken, E. Lopez-Saavedra, A. B. Morelock, J. F. Perello, I. Wiedenhöver, and N. Keeley, Phys. Rev. C 103, 044615 (2021).

^[11] D. Blankstein et al., Nucl. Instrum. Methods Phys. Res. Sect. A 1047, 167777 (2023).

^[12] L. Foreman, P. Kleban, L. D. Schmidt, and H. T. Davis, Phys. Rev. A 23, 1553 (1981).

^[13] J. E. Johnstone *et al.*, Nucl. Instrum. Methods Phys. Res. Sect. A 1025, 166212 (2022).

^[14] Y. Eyal, M. Beckerman, R. Chechik, Z. Fraenkel, and H. Stocker, Phys. Rev. C 13, 1527 (1976).

^[15] A. Hertz, H. Essel, H. J. Körner, K. E. Rehm, and P. Sperr, Phys. Rev. C 18, 2780(R) (1978).

^[16] P. F. F. Carnelli *et al.*, Nucl. Instrum. Methods Phys. Res. Sect. A 799, 197 (2015).

^[17] H. Esbensen, Phys. Rev. C 85, 064611 (2012).

^[18] C. Simenel, R. Keser, A. S. Umar, and V. E. Oberacker, Phys. Rev. C 88, 024617 (2013).

^[19] V. Singh, J. Vadas, T. K. Steinbach, B. B. Wiggins, S. Hudan, and R. T. deSouza, Phys. Rev. C 103, 064606 (2021).

^[20] M. Dasgupta, D. J. Hinde, N. Rowley, and A. M. Stefanini, Annu. Rev. Nucl. Part. Sci. 48, 401 (1998).

^[21] R. J. Tighe, J. J. Kolata, M. Belbot, and E. F. Aguilera, Phys. Rev. C 47, 2699 (1993).

^[22] S. Hudan, R. T. deSouza, A. S. Umar, Z. Lin, and C. J. Horowitz, Phys. Rev. C 101, 061601(R) (2020).